Probing biological interactions one molecule at a time

Brouwer, I.

2016

document version
Publisher's PDF, also known as Version of record

1 General introduction

Ineke Brouwer

1

1.1 Using physics to understand the building blocks of life

In this first chapter I will attempt to introduce the general audience to the concepts that will be described in greater detail in the rest of this thesis. This thesis is written in the field of single-molecule biophysics. Here, a physicist's approach is used to study biology and biological processes at the level of individual molecules, ultimately aimed at understanding as much as possible about life through understanding its individual building blocks. This chapter will start with a brief introduction into the relevant biological topics. First, the biomolecules of interest will be introduced and subsequently the processes in which they are involved. The second part of this chapter focuses on the techniques used to study these processes: optical trapping - used to hold individual molecules in place and to exert forces on them - , fluorescence microscopy - used for direct visualization and localization of biomolecules - and microfluidics - used to directly control the environment of the biomolecules during the experiments. Finally, this chapter concludes with a brief outline of the rest of the thesis.

Cells

All living organisms are built up of cells. These basic building blocks of life most often range between 1 and 100 μm in size and contain the necessary equipment for the cell to survive and replicate. Cells are enclosed by an outer layer called the plasma membrane, separating the inside of the cell from the outside environment. This membrane consists of a bilayer of lipid molecules.

DNA

DNA (deoxyribonucleic acid) is the carrier of the genetic code of life. It is stored in the nucleus of the cell. Its molecular structure, discovered by Watson and Crick in 1953 [1], consists of two long polymer backbones, twisted around each other to form a double helix (Figure 1.1(A)) of double-stranded DNA (dsDNA). The backbone is built up as a chain of sugar molecules linked by phosphates, each attached to one nucleotide base. There are four different bases: adenine (A), thymine (T), guanine (G) and cytosine (C), the sequence of which determines the genetic code of the DNA. By forming base pairs with bases from the opposite strand, the backbones of the two strands are held together. Base pairs form such that an A is always opposite of a T and a G is always opposite of a C (Figure 1.1(B)) [2]. A G-C basepair is held together by three hydrogen bonds while only two hydrogen bonds form an A-T basepair, making a G-C basepair more stable than an A-T pair.

An individual dsDNA molecule behaves somewhat like a rubber band. When not under tension, it coils up, but when under tension, it can be extended elastically. Previous studies [4, 3] quantified the relation between the extension of a dsDNA molecule and the corresponding force (Figure 1.2). At forces below

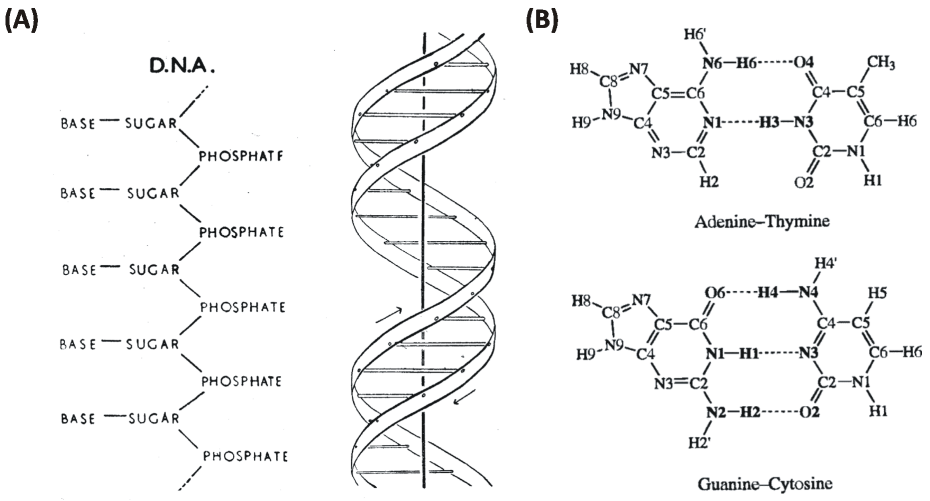

Figure 1.1: The structure of DNA. (A) The chemical structure of DNA consists of a sugar phosphate backbone with a nucleotide base attached to each of the sugar molecules. Figure reprinted from [1]. **(B)** Schematic representation of how the individual strands are held together through hydrogen bonds between opposing bases forming base pairs (indicated by the dashed lines). Figure reprinted from [3].

∼65 pN, DNA behaves elastically. This elastic behavior can be described by the worm-like chain model (WLC; valid ony at very low forces) [5], the extensible worm-like chain model (eWLC; valid up to ∼30 pN) [6] or the twistable worm-like chain model (tWLC; valid up to ∼65 pN) [7]. At forces above ∼65 pN, the basepairing is disrupted and the two strands of the DNA are separated into two individual molecules of single-stranded DNA (ssDNA). This process is referred to as DNA overstretching. The force-extension curve of ssDNA shows a different behavior than dsDNA (Figure 1.2), and can be described with a freely-jointed chain model, as described by Smith et al [8]. In cellular processes such as DNA replication, where the two strands are pulled apart to form templates for two new dsDNA molecules [9], mechanical stress on the DNA leads to the formation of segments of ssDNA. What exactly happens during the transition from dsDNA to ssDNA has long been unclear, but recent work [10] has shown that, if the (local) tension in the DNA reaches overstretching forces, there is a competition between three effects: (1) the DNA strands may separate by starting to unpeel from the ends or from a nick in the DNA, (2) melting bubbles may form, where the DNA strands separate internally, or (3) S-DNA may form, where the DNA is unwound but the basepairs remain intact.

Proteins

Proteins fulfill key functions on the cell, as they are the main regulators of cellular processes such as regulation and signaling. Their basic structure is

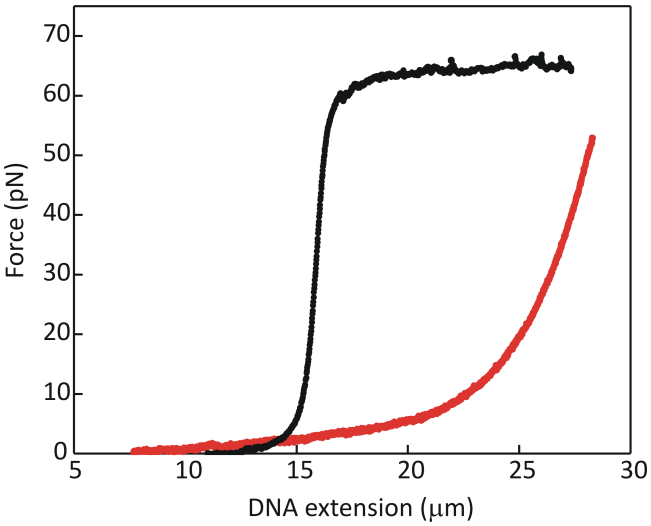

Figure 1.2: Mechanical properties of double- and single stranded DNA. Force-extension curve of a 48.5 kb double-stranded (black dataset) and single-stranded (red dataset) λ DNA molecule.

determined directly by the genetic code of the DNA. Three successive DNA nucleotides encode for one amino acid, the basic building blocks of proteins. There are 20 different amino acids. These amino acids form long chains that fold into 3-dimensional structures, of which the correct folding is often crucial for the function in the cell. Proteins generally fulfill these functions by specifically binding to other biomolecules, such as DNA, membranes and other proteins.

Although each protein is formed from a single unique sequence of amino acids, proteins are not rigid entities with a single conformation or structure. They can be seen as small molecular machines performing specific tasks in the cell, such as the transport of materials, repairing damages or cell signaling. In order to perform these tasks, dynamic transitions between different conformations of the protein are often crucial. In this thesis, we study specific proteins that are involved in protein-mediated membrane fusion (chapter 3) and protein-mediated DNA repair (chapters 4-6).

1.2 Membrane fusion

Membrane-membrane interactions are crucial for cell signaling. For example in brain cells signals are transmitted by the transport of neurotransmitters (chemicals) through the synaptic cleft, the space between cells. These neurotransmitters are packaged in synaptic vesicles, consisting of a lipid bilayer, which can fuse with the receiving cell, releasing the contents of the vesicle on the other side of the plasma membrane (Figure 1.3). The two key steps in this process are the docking of the vesicle to the plasma membrane and the fusion

of the plasma membrane with the synaptic vesicle, forming a new continuous membrane.

Membrane fusion is, in general, triggered by an increase in calcium concentration within the cell and is mediated by a large number of membrane binding proteins. Probably the most famous mediators of membrane fusion are the SNARE complexes [11, 12, 13]. These are large transmembrane complexes that help generate membrane fusion. However, SNARE complexes by themselves are not able to sense elevations in calcium concentrations, so for calcium signaling other factors are needed. Another important group of fusion mediating proteins are C2 domain proteins [14]. These are conserved protein structures that have been identified in more than 200 mammalian cells. Typically, they are involved in calcium sensing by binding both calcium and membranes. One of the proteins from this group is Doc2b, which is known to bind both membranes and SNARE complexes in a calcium-dependent manner. It is known to be crucial for regulation of synaptic vesicle fusion. The exact role of Doc2b in membrane fusion is subject of study in chapter 3.

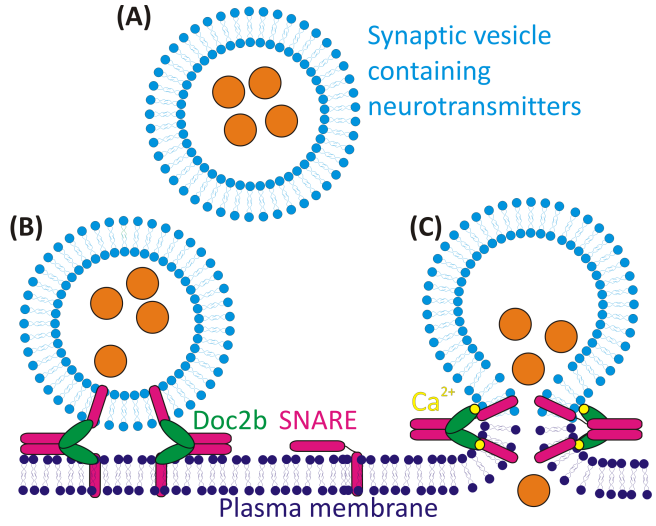

Figure 1.3: Simplified schematic of synaptic vesicles fusing with the plasma membrane mediated by Doc2b and the SNARE proteins. (A) Synaptic vesicle composed of a lipid bilayer containing neurotransmitters. **(B)** Vesicles are positioned at release sites by SNARE-proteins and Ca^{2+} sensors, awaiting a Ca^{2+} trigger. **(C)** Protein-mediated membrane fusion and release of neurotransmitters on the other side of the plasma membrane.

1.3 DNA damage and repair

As DNA is the carrier of genetic information, its stability is crucial for the correct functioning of the cell. Therefore, any damages in the DNA need to be repaired quickly and efficiently. DNA damages can be caused by endogenous and

exogenous factors and, if left unrepaired or incorrectly repaired, they can lead to undesired genetic modifications, which could ultimately lead to cell death, mutations or diseases such as cancer [15]. Perhaps the most severe types of DNA damages are DNA double-strand breaks (DSBs), where both DNA strands are cut and the DNA molecule is physically broken up into two distinct fragments. When a DSB occurs, human cells have two main strategies by which this break can be repaired: non-homologous end-joining (NHEJ) and homologous recombination (HR).

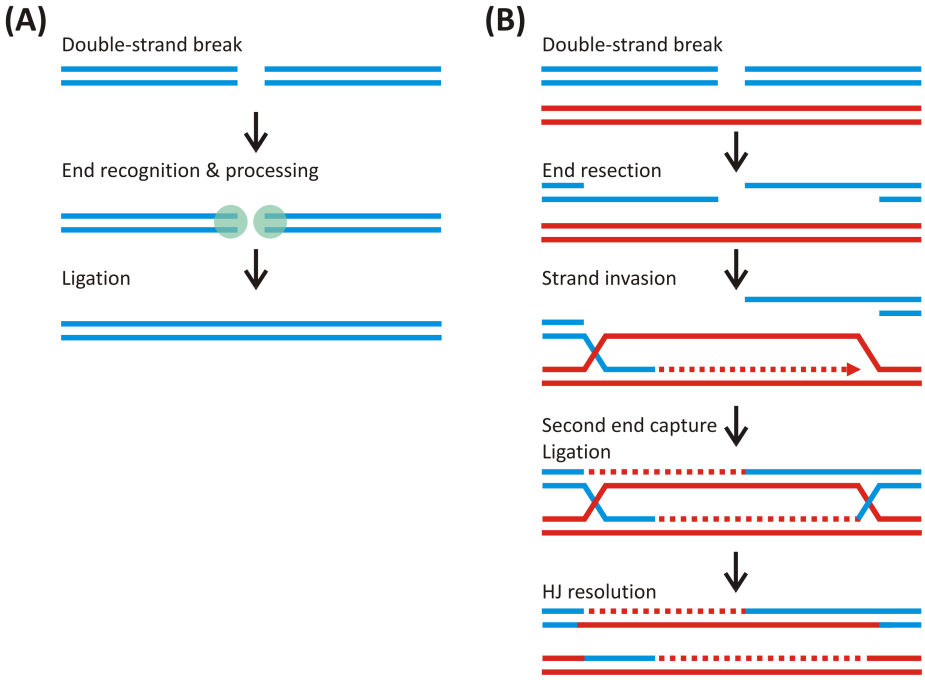

Figure 1.4: Schematic representation of the steps taking place during the repair of double-strand breaks by (A) non-homologous end-joining and (B) homologous recombination.

Non-homologous end-joining

NHEJ is the most prevalent mechanism for repairing DSBs [16]. The main difference between NHEJ and HR is that NHEJ, as opposed to HR, does not depend on the presence of a second copy of the genetic material. Instead, it acts by direct ligation of the broken ends (Figure 1.4(A)). Compared to HR, NHEJ is, however, more prone to errors that may lead to chromosomal translocations, when for example the wrong ends are ligated together or segments of the DNA are missing. The most important players of NHEJ are Ku70/80, DNA-PKcs (both thought to be involved in recognition and processing of the broken ends

[17]), XRCC4, XLF (together thought to be involved in forming an initial connection between the fragments, see chapter 4) and Ligase IV (thought to be responsible for ligation of the ends [17]).

Homologous recombination

HR is a complicated, multistep process involving many different proteins [18, 19]. The main difference between HR and NHEJ in repairing DNA DSBs is that in HR, genetic information is restored by making use of a second copy of the genetic information, stored in the sister chromatid. Correct execution of HR is crucial for maintaining genetic integrity, as can be seen from the fact that malfunctioning of HR-related proteins is can be linked to a variety of cancer syndromes [15].

The most important steps of HR are illustrated in Figure 1.4(B). Briefly, a DSB is formed and detected. Then, the ends are resected to create long ssDNA overhangs. Subsequently, strand invasion and strand exchange occur, by pairing with the sister chromosome. Then, the other DNA fragment is captured and the missing nucleotides are restored through ligation, forming a Holiday Junction (HJ). Finally, the HJ is resolved and the DSB is completely repaired. Well-known key players in this process are replication protein A (RPA, which binds to the ssDNA overhangs after resection to prevent it from being degraded) and RAD51 (which forms a nucleoprotein filament responsible for strand invasion and strand exchange, see also chapter 6). In addition, RAD52 (see chapter 5) might play a role in annealing of the broken strands and second-end capture.

1.4 Single-molecule experiments: biology one molecule at a time

This thesis focuses on studying the biological processes described in the first part of this introduction at the molecular level. To do this, tools are needed with which individual biomolecules can be manipulated, probed mechanically and visualized. In recent years, great efforts have been made to develop techniques to perform single-molecule experiments. Here, I have used a combination of optical trapping, fluorescence microscopy and microfluidics to study interactions between individual biomolecules that are key players in membrane fusion and the repair of DNA damages.

Optical trapping

The basic principle of optical trapping is to use a tightly focused laser beam to hold a particle in place. Once a particle is trapped, we can then move the focus to manipulate the position of the particle. At the same time, the forces acting on the trapped bead can be measured. The force that holds the particle in the focus is a combination of an axial gradient force, driving the particle towards the center of the focus in the direction parallel to the laser beam, and a lateral gradient force, driving the particle towards the center of the focus in

the plane perpendicular to the laser beam. These forces can be understood qualitatively using a ray optics description (Figure 1.5).

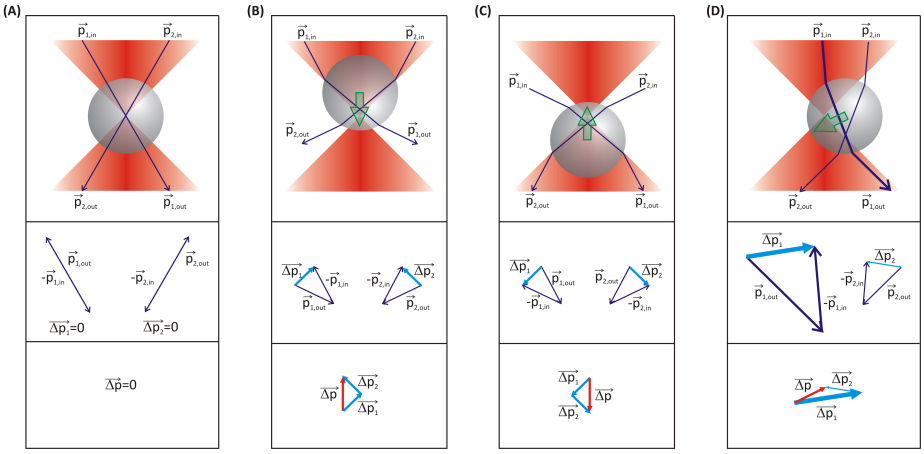

Figure 1.5: Physical principle of optical trapping. Ray optics description of an optically trapped bead. Incoming rays $\mathbf{p}_{1,in}$ and $\mathbf{p}_{2,in}$ are refracted into $\mathbf{p}_{1,out}$ and $\mathbf{p}_{2,out}$ leading to corresponding light momentum changes $\Delta\mathbf{p}_1$ and $\Delta\mathbf{p}_2$. **(A)** If the particle is in the focus, there is no net light momentum change ($\Delta\mathbf{p}$) acting on the bead and it will thus remain in the focus. **(B),(C)** If the bead is pulled out of the focus in the axial direction by an external force, there is a net momentum change of the light and a corresponding restoring force driving the bead back to the focus. **(D)** If the bead is pulled out of the trap in lateral direction, the intensity difference between the incoming rays leads to a net momentum change and a corresponding force driving the particle back towards the focus in the lateral direction.

If a bead is trapped exactly in the laser focus (Figure 1.5(A)), incident rays $\mathbf{p}_1$ and $\mathbf{p}_2$ pass through the center of the bead and thus are not refracted. Therefore, the total light momentum change is zero; there is thus no resultant force acting on the bead. If, however, the bead is displaced out of the trap by an external force in lateral direction (Figure 1.5(B),(C)), the intensities of the incident rays $\mathbf{p}_1$ and $\mathbf{p}_2$ no longer pass through the center of the bead and are thus refracted. This leads in a net light momentum change and thus a net reaction force on the bead in the direction of the highest intensity. In the axial direction, multiple forces act on the bead in the trap. The scattering force of the laser light drives the bead out of the focus. The axial gradient force counteracts this force. Therefore, the particle is only stably trapped if the axial gradient force is larger than the scattering force. If the particle is pulled out of the laser focus in the axial direction (Figure 1.5(D)), this results in a net light momentum change in that same direction, and thus a net reaction force on the bead in the opposite direction, i.e. restoring the particle back towards the laser focus.

To achieve an axial gradient force larger than the scattering force, a tight laser focus is needed, such that a large fraction of the incident light comes from a large incident angle. The maximum angle of incidence is determined by the numerical aperture of the objective and the refractive index of the medium. The maximum force that can be achieved with an optical trap can be increased by

increasing the maximum incident angle (by using an objective with a high NA) or by increasing the laser power.

The forces exerted on a bead in an optical trap can be measured indirectly through the scattering of the trapping laser by the bead. An external force will pull the bead out of the center of the trap, leading to a change in the scattering of the laser light. All light is collected by a condenser lens and imaged on a position sensitive device (PSD) in the back focal plane (BFP) of the condenser lens (Figure 1.6(A)) [20]. The intensity distribution in the BFP only depends on the lateral position of the bead, and is independent of changes in the position of the laser focus in the z-direction.

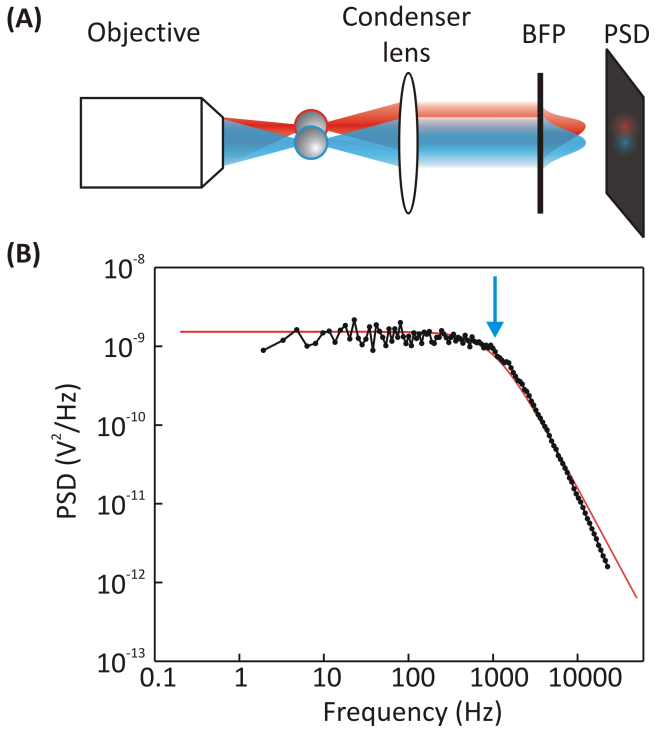

Figure 1.6: Detection and calibration of trapping forces. (A) Configuration of back-focal plane force detection, consisting of microscope objective, trapped bead, condenser, back focal plane (BFP) and position sensitive device (PSD). Displacement of the bead from the center of the trap leads to a change in intensity distribution in the BFP, which is imaged on the PSD. **(B)** Typical power spectrum of a trapped bead with a diameter of 4.5 µm. Data is shown in black and red shows Lorenzian fit, with a corner frequency of 1.02 kHz (as indicated by the arrow). This corresponds to a trap stiffness of 0.27 pN/nm.

The intensity distribution detected on the PSD is measured in Volts, and should therefore be calibrated to determine the signal in units of force. In general, this calibration can be obtained using a known force acting on a trapped bead and measuring the detector response corresponding to this force. The known forces that were used in the experiments described in this thesis were

the Brownian forces acting on a trapped bead. These forces are random, and are counteracted by the optical restoring force described above. The power spectral density of the PSD signal of a trapped bead under the influence of Brownian motion is shown in Figure 1.6(B). From a Lorentzian fit to this data, the corner frequency (blue arrow in Figure 1.6(B)) is obtained. This corner frequency is directly related to the trap stiffness and thus allows for conversion of the PSD signal into units of force [20].

In this thesis, experiments are done using either dual optical trapping or quadruple optical trapping. In dual-trapping experiments, a single trapping laser is split into 2 perpendicular polarizations to create two spatially separated traps that can be manipulated and detected independently. Force detection is possible on one of the two traps. This dual-trap configuration is used to hold the two ends of a single molecule of DNA (chapters 4, 5 and 6) when studying the interaction of specific proteins with the DNA or to hold two membrane-coated beads to study protein-mediated membrane fusion (chapter 3). In quadruple-trap experiments, a single trapping laser is split into four independently steerable laser beams. One of the traps has a unique polarization, allowing force detection on this trap. Force detection on a second trap is achieved by imaging the intensity distribution of a second laser (with a slightly different wavelength) that is coaligned with one of the traps on a second PSD (for a more elaborate description of quadruple-trapping, see chapter 2). In this thesis, this quadruple trap configuration has been used to manipulate the four ends of 2 individual DNA molecules to study protein-mediated DNA-DNA interactions (chapter 4).

Fluorescence microscopy

Fluorescence microscopy is a tool that can be used to visualize objects that are normally too small to be seen under an optical microscope with a resolution on the order of the wavelength of visible light (in the range of 300 to 700 nm) [21]. For example, the width of a DNA molecule is only around 2 nm, and the typical size of a protein is in the order of 10 nm. Nevertheless, these objects van be visualized using fluorescence techniques.

Fluorescence is a process in which a photon of a specific wavelength is absorbed, and subsequently a photon of a longer wavelength is emitted. The change in wavelength between the absorbed and the emitted photon (the Stokes shift) is caused by the loss of energy between absorption and emission of the photon. In general, the intensity of the emitted fluorescence signal is very weak: for excitation intensities in the order of W/cm^2, fluorescence intensities are in the order of fW [22]. Still, this fluorescence light can be discriminated from the excitation light using a suitable dichroic mirror and then collected on a CCD camera. The major limitation of fluorescence microscopy is photodamage: when a fluorescent dye is exposed to high-intensity excitation light, it will only emit in the order of 10^5-10^6 photons before the fluorophore is damaged by the excitation light [22]. After this, the fluorophore transitions into a dark energetic state, where it no longer fluoresces. This process is referred to as photobleaching.

In this thesis, two different implementations of fluorescence microscopy have

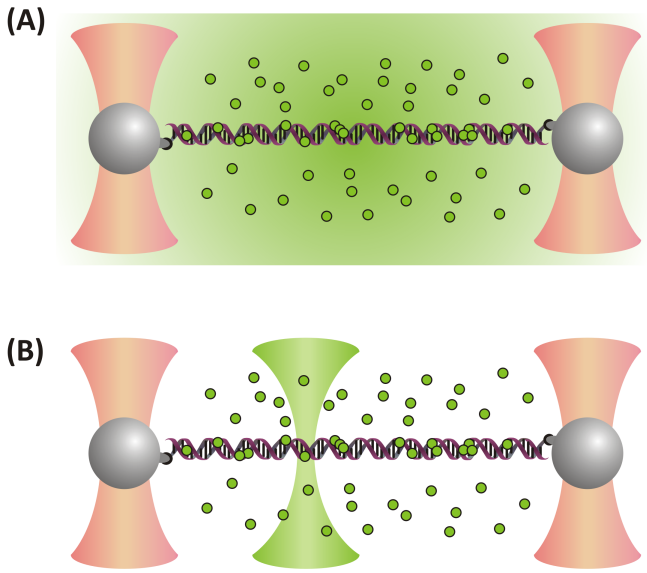

Figure 1.7: Wide field and confocal fluorescence microscopy. (A) Schematic representation of wide field fluorescence microscopy, where the entire field of view is illuminated with a fluorescence excitation laser. Therefore, all fluorophores that are on proteins in solution or on DNA-bound proteins emit fluorescence, leading to a large background signal. **(B)** Schematic representation of confocal fluorescence microscopy, where a focused fluorescence excitation laser is used, there, thus only exciting the small fraction of the fluorophores that is within the confocal volume emits fluorescence.

been used: wide field fluorescence microscopy and confocal fluorescence microscopy. In wide field fluorescence, the entire field of view is illuminated, and all fluorescent probes within this field of view fluoresce (Figure 1.7(A)), including those that are in solution, leading to a large background signal. In general, this means experiments cannot be performed directly in a solution with a high concentration of (fluorescently labeled) proteins. In confocal fluorescence microscopy, on the other hand, the fluorescence excitation laser is focused within a much smaller region, exciting only the fluorescent probes within this confocal spot. This allows the fluorescence signal to be measured in much higher concentrations of fluorescent probes in solution. In our implementation, we scan the confocal spot along a biomolecule that is tethered between the beads (Figure 1.7(B)). A drawback of confocal fluorescence is that, since the effective excitation power at the excitation focus is much higher, photobleaching occurs faster than in wide field configuration.

Combining optical trapping and fluorescence microscopy

Optical trapping can be combined with simultaneous fluorescence microscopy, creating a more powerful biophysical technique as the locations of fluorescence events and the forces are measured simultaneously. A typical process that can

be studied using this technique is the binding of (fluorescently labeled) proteins to DNA, where the effect of binding is measured in the force signal while the location of the enzyme along the DNA and the number of proteins bound are determined using the fluorescence photons the protein emits. This combination of techniques was first achieved by Ishijima et al [23]. Several other labs have aplied similar techniques since [24, 25]. The main drawback of combining these techniques is that the trapping laser enhances photobleaching of the fluorophores [22], especially at higher trapping powers or fluorescence excitation powers. This effect is even larger in the case of confocal fluorescence excitation, because of the higher excitation power used. Several efforts have been made to reduce this effect, such as the use of antioxidants or oxygen-scavenger systems or by separating the trapping and fluorescence excitation light in time [26] or in space [27, 28]. The latter can be achieved by using relatively large microspheres, such that the focus of the trapping laser is far away from the fluorophores.

The DNA, proteins and lipids used for the experiments described in this thesis are not naturally fluorescent. Therefore, the proteins and lipids can be fused to fluorescent probes with fluorescence properties. 6 different fluorescent probes are used throughout this thesis, of which the fluorescence spectra are shown in Figure 1.8. The probes eGFP, Fluorescein, Alexa Fluor 488, and NBD can be excited using a blue (491 nm) fluorescence excitation laser. Alexa Fluor 555 can be excited in green (532 nm) and Atto 647N in red (639 nm).

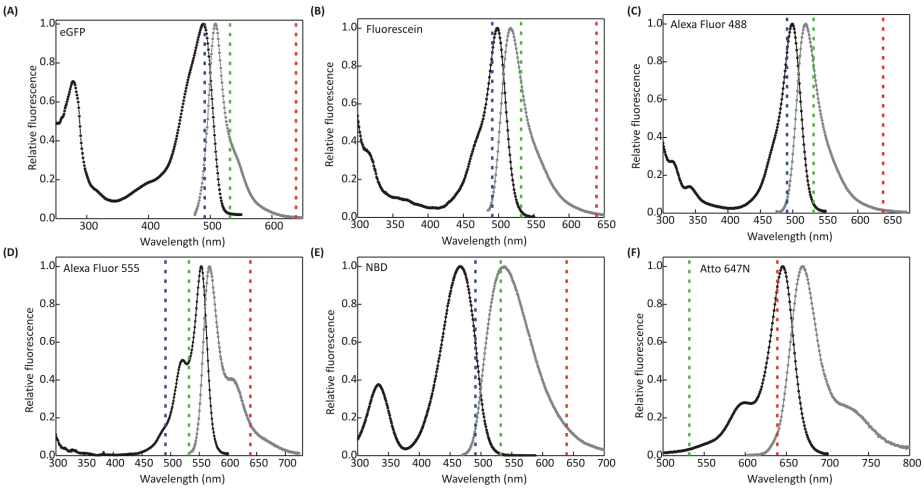

Figure 1.8: Excitation and emission spectra of fluorescent probes used in this thesis. (A) eGFP **(B)** Fluorescein **(C)** Alexa Fluor 488 **(D)** Alexa Fluor 555 **(E)** NBD **(F)** Atto 647N. Black: normalized excitation spectrum, grey: normalized emission spectrum, blue: location of the 491-nm blue excitation laser, green: location of the 532-nm green excitation laser, red: location of the 639 nm red excitation laser.

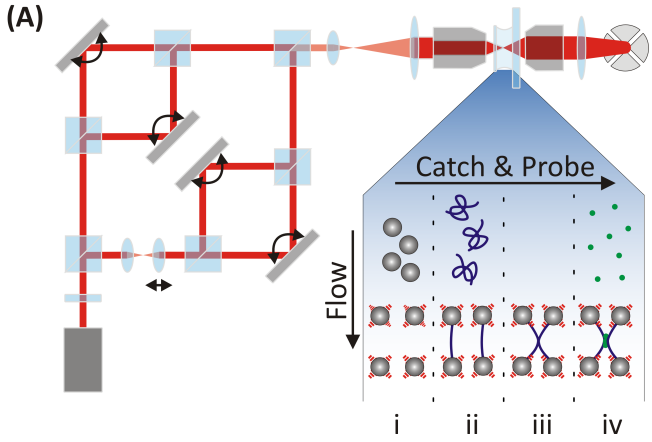

Figure 1.9: Schematic representation of the experimental setup used. Four optical traps are generated from a single laser. The position of each trap can be individually controlled using piezo-driven mirrors. DNA molecules or other biological constructs can be caught (i-ii), tested (iii) and measured (iv) in a multi-channel laminar flow cell. Figure adapted from [30].

Microfluidics

Single-molecule optical trapping experiments require precise temporal and spatial control of the biomolecules and their chemical environment. It is necessary to be able to switch between different environments relatively easily and quickly. To achieve this, our experiments were performed in a microfluidic flow cell. This flow cell consists of up to six channels. The different solutions flow simultaneously, joining into a larger channel containing laminar flows where different solutions flow and experiments are performed (Figure 1.9). Its total volume is approximately 80 μL. The advantage of such a laminar system is that it enables fast buffer exchange, making experiments relatively easy and fast. Mixing between the channels only occurs within a few microns of the immediate fluid interface, even for entry channels perpendicular to the main channel [29].

Preparation of reagents

In the experiments described in this thesis, biomolecules were attached to polystyrene microspheres, which could be held in optical traps. For the experiments with DNA and DNA-binding proteins (chapters 4, 5 and 6), DNA constructs were made by modifying λ DNA to attach multiple biotin molecules to both ends of the DNA molecules (Figure 1.10). These biotin molecules bind tightly to streptavidin molecules, and can thus be used to link the DNA molecules to the streptavidin-coated microspheres. For experiments with double-stranded DNA, biotin molecules were attached to the 5′ ends of both DNA strands, while for experiments with single-stranded DNA, biotin molecules were attached to both the 3′ and the 5′ end of the same DNA strand. Single-stranded

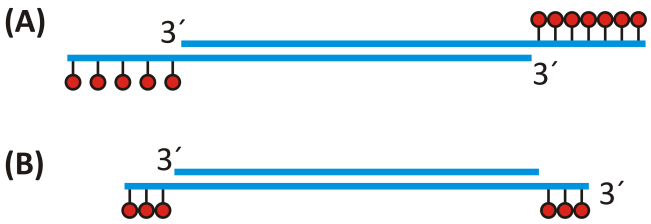

Figure 1.10: Schematic representation of DNA constructs used for experiments involving DNA-protein interactions. Both constructs are based on the 48.5-kb λ DNA molecule, where the ends are modified to attach biotins on (A) both strands for dsDNA experiments or (B) only the bottom strand for ssDNA experiments.

DNA could then be generated by force-induced melting. For the experiments on membrane fusion (chapter 3) the polystyrene microspheres were coated with a lipid bilayer to mimic the membrane and the vesicles during the fusion process (Figure 1.11).

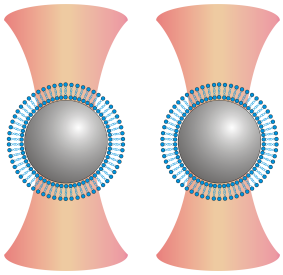

Figure 1.11: Schematic of optically trapped lipid-coated polystyrene beads for studying membrane fusion.

1.5 Outline of this thesis

Chapter 2 describes how to perform a quadruple-trap optical tweezers experiment. A step-by-step guide is provided of how to perform such an experiment, which could, for instance, be used to study the protein-mediated interactions between 2 individual DNA molecules (such as the interactions that will play a central role in chapter 4). In addition, this chapter includes a detailed description of the optical setup used and protocols for cleaning and passivating of the microfluidic devices in which the experiments are performed.

In **Chapter 3** we present a novel application of our approach combining dual optical trapping and fluorescence microscopy to study membrane fusion between two membrane-coated microspheres. We use this method to study the role of the calcium sensor Doc2b in membrane fusion and show that in the presence of calcium and Doc2b, the outer layers of the lipid bilayers on the beads fuse,

while the inner layer remain intact. This forms a highly force-resistant structure: membrane hemifusion.

Chapter 4 presents the study of the interaction of DNA with XRCC4 and XLF, two crucial proteins for DNA repair by non-homologous end-joining. Here, we used both dual optical trapping combined with confocal fluorescence microscopy and quadruple trapping combined with wide field fluorescence microscopy to unravel the mechanism of action of XRCC4 and XLF. We show that XLF binds DNA in a highly cooperative manner and at the same time stimulates the binding of XRCC4 and XRCC4-XLF complexes to DNA. These complexes bind DNA in a highly diffusive and mobile manner. XRCC4-XLF complexes can form bridges between fragments of broken DNA, holding them together and preparing them for further processing in the repair pathway.

Chapter 5 focuses on a different DNA repair protein: RAD52, a component in DNA repair by homologous recombination. We show that RAD52 interacts with both single- and double-stranded DNA. On ssDNA, we find a tight binding where the ssDNA wraps around complexes of RAD52. On dsDNA, we observe a weaker and often diffusive binding. The mobility of RAD52 along the DNA might suggest it is able to recognize stretches of ssDNA or DNA damages. In addition, binding of RAD52 to dsDNA profoundly alters its mechanical properties by greatly enhancing DNA flexibility and slightly increasing the DNA length. Finally, the nature of the overstretching transition of dsDNA changes drastically in the presence of RAD52, in a manner that might be advantageous for holding two two strands of ssDNA together during or after their annealing, a key step in DNA repair by homologous recombination.

In **chapter 6** the protein RAD51 is studied, a protein that plays a crucial role in homologous recombination. RAD51 forms filaments on ssDNA that are responsible for performing strand-exchange. Using our setup, we can directly monitor how long these proteins remain bound to the ssDNA and show that this is dictated by the ability of the bound ATP to hydrolyze. In addition, we can probe the elastic response of these filaments and show that ATP-bound filaments can be in one of two conformations with different lengths. The free energy difference between these two states is around 4 k_BT, and transitions between the states can be triggered by tension. When ATP hydrolyzes, the filament converts into a single ADP-bound configuration, from which it can disassemble. Finally, we study the effect of BRC4, a domain of the BRCA2 protein that is a known regulator of RAD51, on these filaments. We show that, under our experimental conditions, the interaction between BRC4 and RAD51 must be very short-lived, but can significantly slow down both the formation and the dissociation of the filaments. These insights may be a first step in understanding the structure, kinetics and regulation of RAD51 filaments.